ALMA MATER STUDIORUM
UNIVERSITÀ DI BOLOGNA

ARCHIVIO ISTITUZIONALE
DELLA RICERCA

Alma Mater Studiorum Università di Bologna
Archivio istituzionale della ricerca

The Challenging Conformational Landscape of Cysteamine···H2O Revealed by the Strong Interplay of Rotational Spectroscopy and Quantum Chemical Calculations

This is the final peer-reviewed author's accepted manuscript (postprint) of the following publication:

Published Version:
Song, W., Maris, A., Cummings, C.N., Evangelisti, L., Walker, N.R., Melandri, S. (2024). The Challenging Conformational Landscape of Cysteamine···H2O Revealed by the Strong Interplay of Rotational Spectroscopy and Quantum Chemical Calculations. THE JOURNAL OF PHYSICAL CHEMISTRY LETTERS, 15(40), 10054-10061 [10.1021/acs.jpclett.4c02353].

Availability:
This version is available at: https://hdl.handle.net/11585/1003116 since: 2025-01-26

Published:

DOI: http://doi.org/10.1021/acs.jpclett.4c02353

Terms of use:

Some rights reserved. The terms and conditions for the reuse of this version of the manuscript are specified in the publishing policy. For all terms of use and more information see the publisher's website.

This item was downloaded from IRIS Università di Bologna (https://cris.unibo.it/).
When citing, please refer to the published version.

(Article begins on next page)

14 September 2026

The Challenging Conformational Landscape of Cysteamine···H_2O Revealed by the Strong Interplay of Rotational Spectroscopy and Quantum Chemical Calculations

Wentao Song, Assimo Maris, Charlotte N. Cummings, Luca Evangelisti, Nicholas R. Walker,* and Sonia Melandri*

ABSTRACT: A 1:1 molecular complex of cysteamine with water is shown to adopt a cage-like structure where cysteamine accepts a relatively strong hydrogen bond from water while also engaging in two additional weaker interactions (SH···O_w and CH···O_w). Experimental and theoretical approaches confirm this conformer as the global minimum on the potential energy surface. Fitting of key structural parameters to experimentally determined moments of inertia yields consistent and accurate results for rotational and ^{14}N nuclear quadrupole coupling constants which are shown to be challenging to calculate using *ab initio* methods. Comprehensive analysis of the intermolecular interactions and a thorough comparison with the properties of aminoethanol−water is presented, utilizing independent gradient models based on Hirshfeld partition, quantum theory of atoms-in-molecules, and symmetry-adapted perturbation theory approaches. As expected, the OH group of aminoethanol is a stronger hydrogen bond donor than the SH group in cysteamine, while the CH···O_w interaction is a key determining factor of the conformational landscape in both cysteamine−water and aminoethanol−water complexes. The results show very clearly that the synergy between theoretical calculations and experimental results is not only desirable but mandatory to get the right answers in such complex conformational surfaces. The results are also clear benchmarks for the accuracy of different theoretical methods in assessing the structures and energy order of the conformations.

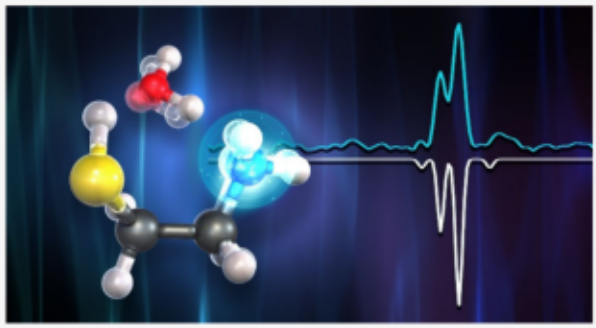

Life is sustained by a dynamic balance of biochemical processes that are critically mediated by water. Changes in conformation that accompany solvation by water have the potential to strongly influence the activity and bioavailability of molecules.[1] Intra- and intermolecular interactions which are important in bulk water solutions[2,3] can be studied through a combination of accurate theory and spectroscopic experiments performed on small clusters in the gas phase. Within such clusters, the presence of multiple, competing binding sites for non-covalent interactions (NCIs) typically leads to shallow potential energy surfaces (PESs), low barriers to conformational isomerism and large amplitude motions.

Rotational spectroscopy is a uniquely powerful method by which structural parameters can be determined with high precision and size-selectivity for gas phase complexes.[4] It is possible to isolate and accurately characterize multiple conformers simultaneously where they are generated under the chosen experimental conditions. The technique thus allows for detailed exploration of the competition and/or cooperativity that can exist between NCIs present within an isolated molecular complex. The conformational isomerism that results from the interplay between NCIs is very challenging to model theoretically.[5] In the present work, conformational isomerism within the 1:1 gas phase molecular complex formed between cysteamine and water (hereafter termed CYS−W) has been studied to reveal exquisite details of the competition between individual C−H···O_w, S−H···O_w and N···H−O_w NCIs which are of broad importance in a wide variety of biochemical environments.[6,7]

Our previous study characterized five conformers of the cysteamine (alternatively referred to as 2-mercaptoethylamine or 2-aminoethanethiol, CYS) monomer which are distinct from each other by virtue of the intramolecular NCIs they contain.[8] CYS is an aminothiol endogenously synthesized by human body cells during the coenzyme A metabolism cycle and constitutes a part of its frame.[9−12] CYS serves as a medicinal agent with a wide range of applications in the treatment of various medical conditions.[13−20] However, its

applications may be constrained by its substantial hygroscopicity and other characteristics which derive from the multiple hydrophilic functional groups which are positioned and oriented to allow CYS to interact with water solvent. Moreover, the consequences of hydrogen bonding to S−H groups in biochemical systems, and the differences between hydrogen bonds formed to S−H and O−H groups are a matter of current interest.[21] While very important in the context of biochemistry, the interaction between water and each of CYS and its oxygenated analogue aminoethanol (AE) is also significant to our evolving understanding of chemical processes on icy grain surfaces in the interstellar medium.[22]

Binding of water to a small, flexible molecule can disrupt intramolecular NCIs and prompt conformational change.[23,24] Conversely, water may simply add to the exterior of a molecule without having such effects.[23,25−27] A preliminary screening of the conformational space available to CYS−W was performed using the Conformer-Rotamer Ensemble Sampling Tool program (CREST)[28] which uses a metadynamic-driven search algorithm on a tight binding semiempirical PES. This led to 419 structures which were subsequently optimized based on density functional theory (DFT, B3LYP-D3(BJ)/Def2-TZVP) and 39 nonequivalent conformers were identified. The described diversity of conformers exists because CYS is conformationally flexible and moreover offers multiple sites to which H_2O can bind. More details on computational calculations and the structures found by CREST and optimized by DFT are shown in Figure S1 of the Supporting Information (SI) together with relative energies, rotational constants and electric dipole moments.

Subsequent to the B3LYP optimizations, *ab initio* geometry optimizations were performed for the five most stable conformers at the MP2/aug-cc-pVTZ level of calculation. These yielded the four structures depicted in Figure 1 with the relative energy values $\Delta E_e/\Delta E_0$ (ΔE_e is the relative electronic energy and ΔE_0 is the zero-point corrected relative energy) and intermolecular binding distances as given. A three-letter code is used to characterize the different conformations of CYS in the water complexes, where the *g* (*gauche*), *t* (*trans*), and *g′* (*gauche′*) letters are related to the different values of the HS−C2C1, SC2−C1N, and (lp)N−CC rotatable dihedral angles in this order. Low-energy conformers are characterized by a hydrogen bond (HB) between the hydroxyl group of water and the lone pair of the amine where the bond length is approximately 1.9 Å consistent with a strong HB.[29] The two most stable conformations are #A (global minimum) and #B which has a zero-point corrected relative energy of 1.2 kJ mol^{-1}. In #A, water creates a bridge between the amino and thiol groups of CYS acting as proton donor (d_{N-HO} = 1.895 Å) and proton acceptor (d_{O-HS} = 2.395 Å), respectively. Moreover, an additional short distance is found between the water oxygen and the CH group adjacent to the thiol group (d_{O-HC} = 2.541 Å). Conformer #B, besides the N···HO hydrogen bond (d_{N-HO} = 1.895 Å), shows an interaction of the water oxygen to the CH group adjacent to the thiol group (d_{O-HC} = 2.459 Å). Notably, both for #A and #B, the CYS frame does not assume the global minimum conformation of the isolated species (*gGt*) but that of the higher energy arrangements, *g′Gg* and *gGg*.[8] The *gGt* arrangement can still be observed in a conformer with relatively higher energy, labeled as #C, where water interacts with the amine lone pair (d_{N-HO} = 1.908 Å) without destroying the intramolecular NH···S interaction (d_{NH-S} = 2.749 Å). In regards to #D, CYS assumes

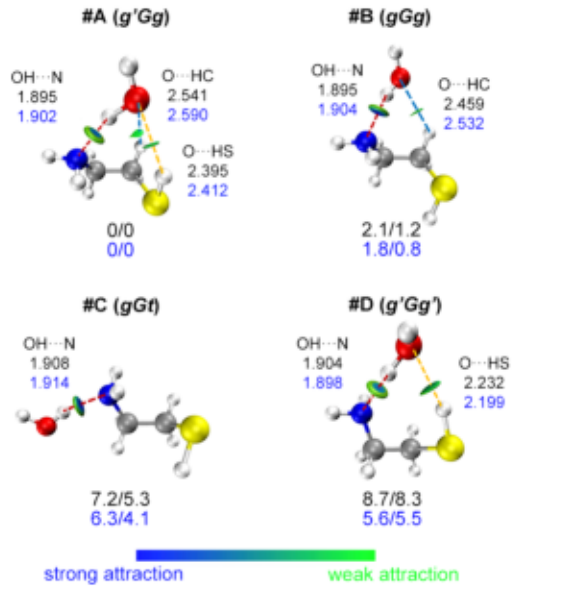

Figure 1. Theoretical (MP2/aug-cc-pVTZ) structures, HB distances (*d* in Å) and relative energy values ($\Delta E_e/\Delta E_0$ in kJ mol^{-1} where ΔE_e is the relative electronic energy and ΔE_0 is the relative zero-point corrected relative energy) of the four more stable conformers of CYS−W; the parameters in black are the ab initio values, while those in blue are the DFT values. Labels in parentheses describe the *trans*, *gauche*, or *gauche′* arrangements of the HS−CC, SC−CN, and (lp)N−CC dihedral angles in this order. The isosurfaces are from independent gradient models based on Hirshfeld partition calculation (isovalue of δ_g = 0.01 a.u.; δ_g is a function of electron density gradient reflecting the interaction) and colored on a BGR scale corresponding to the value of sign(λ_2) (ρ is the actual electron density of the current system).

a *g′Gg′* conformation and water creates a bridge between the amino and thiol groups of CYS as in #A while the intermolecular distances are d_{N-HO} = 1.904 Å and d_{O-HS} = 2.231 Å. It is worth noting that the second most stable conformer from the DFT calculation (#A′, whose structure is shown in Figure S1), which transfers to #A at the MP2/aug-cc-pVTZ level of calculation, differs from #A only because of the orientation of the hydrogen atom of water not involved in intermolecular interactions.

Rotational spectroscopy experiments were conducted using two complementary instruments, the high-resolution cavity-based pulsed jet Fourier transform microwave (PJ-FTMW) spectrometer in Bologna[30−33] and the broadband chirped pulse Fourier transform microwave (CP-FTMW) spectrometer in Newcastle.[34] Details of the theoretical and experimental methods as well as of the Hamiltonian employed and the list of measured lines (Tables S1 and S2) are provided in the SI. The assignment and analysis of spectroscopic transitions were performed using the CALPGM software.[35] The parameters thus determined are the rotational constants *A*, *B* and *C*; the quartic centrifugal distortion parameters, D_J, D_{JK}, D_K, d_1 and d_2; and the nuclear quadrupole coupling (NQC) constants for the ^{14}N nucleus, χ_{aa}, χ_{bb} and χ_{cc}. The latter were determined by analysis of characteristic hyperfine splittings such as those illustrated in Figure 2 and all constants are reported in Table 1.

Comparison of the experimentally determined and theoretically calculated rotational constants confirms that the observed species of CYS−W has the conformation of #A while detailed analysis (see Table S3) shows that the *ab initio*

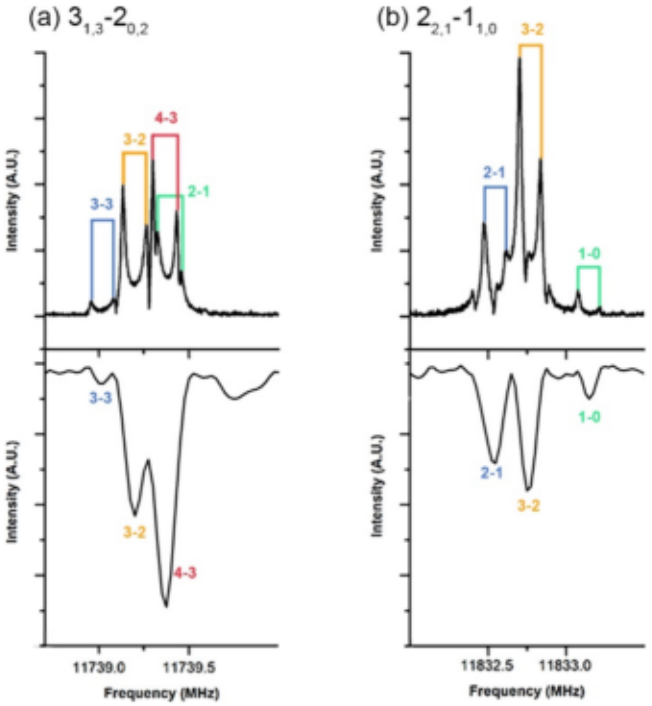

Figure 2. Resolved nuclear hyperfine structure of the $3_{1,3} - 2_{0,2}$ (a) and $2_{2,1} - 1_{1,0}$ (b) rotational transitions. Each hyperfine component is annotated with the respective values of F' and F quantum numbers. The upper part corresponds to the PJ-FTMW data showing the typical Doppler splitting due to the parallel arrangement of the molecular beam and the radiation. The lower part corresponds to the CP-FTMW data: because of the perpendicular alignment of the jet plume and the axis of radiation propagation, the spectral resolution is lower than for the PJ-FTMW spectrometer.

calculated rotational constants are overestimated by 3−5%. The differences between the experimental and theoretical results are high when compared with smaller variations seen previously during studies of similar water-containing complexes.[36] They are greater than implied by the fact that the experimental constants are determined for the zero-point vibrational state (r_0) whereas the theoretical constants are for the equilibrium geometry (r_e). The experimentally determined NQC constants were found to differ significantly from those calculated theoretically, especially for χ_{aa} of CYS−W (see Table S3). The differences limited the value of the theoretical results with respect to the assignment of the rotational spectra. Evidently, complexes formed between conformationally flexible molecules such as CYS with water pose a significant challenge for computational methods. In contrast, calculations performed at the same level of theory for the noncomplexed CYS (Table S4) yielded results for the *g′Gg* conformer that were in good agreement with experimentally determined quantities.[8]

Direct information on molecular structure can be obtained using Kraitchman's substitution method,[37] which, under an assumption that isotopic substitution does not alter molecular geometry, allows the determination of the coordinates (absolute values, relative to the principal inertial axis system of the parent isotopologue) for every atom for which an isotopic substitution is available. Experimental rotational constants (reported in Tables 1 and S5) were used to calculate absolute substitution coordinates of the S and O atoms using this method while Costain's model[38] was used to derive the uncertainties. These are compared to the principal axes coordinates calculated theoretically (r_e) in Table S5. Despite the differences between experiment and theory, the agreement is good enough to further confirm that the observed spectrum should be assigned to conformer #A. In an alternative procedure, starting from a trial geometry (in our case the MP2/aug-cc-pVTZ one), a set of selected internal coordinates was adjusted to reproduce the experimental rotational constants, using a least-squares approach. In particular, we applied Kisiel's STRFIT program[39] to determine a pseudo-r_0 geometry (where r_0 denotes the zero-point vibrational level geometry) by fitting five structural parameters to the experimentally determined rotational constants while holding all others at their values for the calculated r_e geometry. The fitted parameters were the O···S distance (d_{OS}), the ∠OSC1 angle, and the OSC1C2 dihedral angle, which define the position of water oxygen with respect to CYS, and the angles ∠SC1C2 and ∠C1C2N, which describe the skeletal arrangement of CYS. The nine rotational constants of the three observed isotopic species could be reproduced with a standard deviation of 0.5 MHz, providing the parameters shown in Figure S2 and Table S6, where they are compared to the original r_e values. It is worth noting that the r_0 angles of CYS are slightly greater than the equilibrium (r_e) quantities. The same effect is also observed for the derived HB distances, also given in Figure S2, whereby the difference between the r_0 and r_e distances is 0.09 Å for SH−O and 0.06 Å for N−HO, respectively.

After the described fit, a single-point MP2/aug-cc-pVTZ calculation was carried out on the pseudo-r_0 structure obtained for conformer #A to quantify the dependency of the NQC constants on the values of structural parameters. The theoretically calculated NQC constants, reported in the last column of Table 1, are in acceptable agreement with those determined by the approach described above, suggesting that differences between the theoretically calculated and experimentally determined structures also explain the mismatch between the "raw" theoretical and experimental results for the NQC constants. Similar calculations at the same level of theory reproduced the NQC constants observed for other isotopologues (Table S5) despite the fact that there is significant variation in these parameters across the isotopologues studied. The implication is that the pseudo-r_0 structure is reliable and that the effects of changes in zero-point energy on isotopic substitution are negligible.

The experimental structure of CYS−W is similar to that determined for AE−NH_3.[22] Indeed, both complexes are characterized by the smaller ligand inserted into the bidentate alkane in *g′Gg* conformation. However, the orientation of the ligands cannot be compared because of their different symmetry, C_{2v} for water and C_{3v} for ammonia but a more precise comparison can be made for AE−W. For this system, the rotational spectrum of one conformer of the 1:1 complex was previously reported[40] and in a recent paper, three conformations were observed by rotational spectroscopy and assigned with the support of DFT calculations which used both the B3LYP-D3(BJ)/Def2-TZVP and the rDSD//B3 model which combines the rev-DSD-PBEP86-D3BJ/cc-pVTZ-F12 and B3LYP-D3(BJ)/6-31+G* levels of theory to account for vibrational corrections.[41] The lowest-energy conformers of AE−W identified by Xie et al.[41] share many of the structural features of the CYS−W conformers presented in Figure 1. Applying the labeling conventions of the present work to the conformers earlier identified by Xie et al.,[41] however, the

Table 1. Experimental Spectroscopic Parameters of CYS−W, Theoretical (MP2/aug-cc-pVTZ) Parameters of the Most Stable Conformers of CYS−W, and Calculated Parameters at the Pseudo-r_0 Geometry (MP2/aug-cc-pVTZ)

Parameter[a]	Exp.	#A	#B	#C	#D	pseudo-r_0
A (MHz)	3370.994(1)[b]	3408.60	4752.49	8178.77	3277.77	3371.35
B (MHz)	2475.1442(8)	2605.10	1783.31	1201.87	2527.71	2475.41
C (MHz)	1719.8490(5)	1802.74	1571.10	1163.01	1521.89	1719.83
D_J (kHz)	5.27(2)	4.141	4.148	2.582	3.913	—
D_{JK} (kHz)	−14.0(2)	−5.318	−34.003	−90.325	−6.047	—
D_K (kHz)	16.3(1)	2.180	113.042	1194.621	2.754	—
d_1 (kHz)	2.05(2)	0.340	−1.204	−0.060	0.632	—
d_2 (kHz)	—	−0.718	−0.011	0.031	−0.237	—
$1.5\chi_{aa}$ (MHz)	−0.197(5)	0.11	−1.55	−5.5	2.88	−0.20
$0.25(\chi_{bb} - \chi_{cc})$ (MHz)	−0.412(2)	−0.49	−0.95	−0.14	−1.23	−0.37
N	91	—	—	—	—	—
σ (kHz)	6.6	—	—	—	—	—
M_{aa} (uÅ^2)	27.13	24.40	88.53	179.35	22.88	27.13
M_{bb} (uÅ^2)	119.79	115.77	72.31	37.92	143.16	119.80
M_{cc} (uÅ^2)	30.13	29.43	34.03	23.87	11.05	30.10
μ_a (D)	obs.	−1.7	0.3	1.3	0.1	−1.44
μ_b (D)	obs.	2.7	2.8	0.5	3.9	−2.77
μ_c (D)	obs.	0.6	−0.4	1.3	−0.7	−0.59
χ_{aa} (MHz)	−0.131(4)	0.076	−1.032	−3.665	1.919	−0.130
χ_{bb} (MHz)	−0.758(5)	−1.021	−1.377	1.555	−3.420	−0.678
χ_{cc} (MHz)	0.889(5)	0.945	2.409	2.110	1.501	0.808

[a]A, B and C are the rotational constants. D_J, D_{JK}, D_K, d_1 and d_2 are the quartic centrifugal distortion constants. χ_{aa}, χ_{bb} and χ_{cc} are the nuclear quadrupole coupling tensor diagonal elements for the ^{14}N atom. N is the number of transitions in the fit. σ is the standard error deviation of the fit. M_{aa}, M_{bb} and M_{cc} are the planar moments of inertia; these are derived from the moments of inertia (I) as for example $M_{cc} = (I_{aa} + I_{bb} - I_{cc})/2$. μ_a, μ_b and μ_c are the electric dipole moment components; obs. means that the transitions involving the components have been observed. [b]Standard errors in parentheses in units of the last digit.

lowest-energy conformers of AE−W are #D (labeled isomer 1 within ref 37); a variant of #A which is hereafter labeled #A′ (labeled isomer 2 within ref 37); and a higher energy species (labeled isomer 4 in ref 37) where AE adopts a $g'Gg'$ arrangement which retains intramolecular OH−N and H_2O−OH hydrogen bonds and where water bridges the OCCH frame (this conformer will be referred to as #E hereafter). Xie et al.[41] identified isomer 1 as being the global minimum on the PES with other isomers labeled in order of increasing energy relative to this global minimum.

The implication of the apparently different conformer energy orderings of AE−W and CYS−W is that contributions to the overall energy made by the various intramolecular and intermolecular interactions are somewhat different within each complex. In order to verify this picture, we performed additional *ab initio* calculations on AE−W and included conformer #A in our analysis. In Table S7 the MP2/aug-cc-pVTZ results are compared to the experimental and DFT values reported by Xie et al.[41] As regards the relative energies, the main difference in going from B3LYP-D3(BJ)/Def2-TZVP to MP2/aug-cc-pVTZ is that #A, #A′ and #D become much closer in energy, in particular AE−W #A is predicted to be the global minimum, followed by #D (ΔE_e = 0.07 kJ mol^{-1}) and #A′ (ΔE_e = 0.24 kJ mol^{-1}). Also, the relative energy of the observed conformer #E decreases from 11.1 to 5.9 kJ mol^{-1}. As concerns the NQC constants, the agreement between the *ab initio* and the experimental values for #D and #E is quite good, being the absolute values of χ_{aa} and $\chi_{bb}-\chi_{cc}$ underestimated by less than 0.04 and 0.09 MHz, respectively. Unfortunately, neither the NQC values of #A nor those of #A′ match well with the experimental data, but curiously their average values do (within 0.04 MHz).

Measurements of geometrical (or other) parameters determined by microwave spectroscopy are necessarily performed for a molecule or complex in its zero-point vibrational state. In the zero-point vibrational state, the molecular geometry of a complex may rapidly interconvert between different minima that have similar low energy on the PES while a microwave spectroscopy experiment measures only the vibrationally averaged geometry over the time scale of the molecular rotation. For this reason, it is sometimes found that structural parameters determined by microwave spectroscopy may be different from those for the minimum-energy conformation calculated for a molecule using *ab initio* theory or DFT. Rapid interconversion between conformational forms is commonly assumed when analyzing the rotational spectra of complexes that contain either water or an OH group (this is a reasonable assumption only if the energetic barrier to such interconversion is expected to be low). It follows that #A and #A′ of AE−W might rapidly interconvert on the time scale of a microwave spectroscopy experiment.

Energetic barriers to conformer interconversion, and hence the dynamics of conformational isomerism, have been shown to be different in complexes that contain H_2S and/or −SH rather than H_2O and/or −OH.[42] Looking again at the results for CYS−W with reference to the rationale presented above, we can suppose that #A′ is not a minimum on the *ab initio* PES for CYS−W and is instead an inflection point while #A remains the global minimum or that the two minima #A and #A′ could be separated by a small barrier with the ground state lying above the barrier, delocalized on both wells. Nevertheless, the shape of the PES affects the effective structure of the molecule, explaining the discrepancies between the theoretical and the experimental results. It is quite clear that the observed

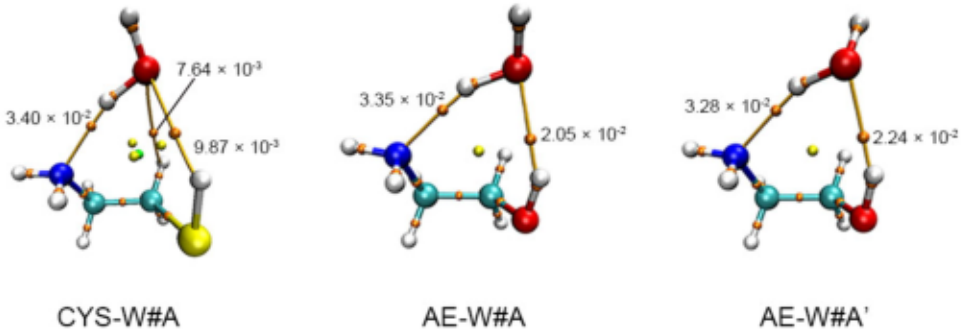

Figure 3. Results from QTAIM analyses for the global minimum of CYS−W#A, AE−W#A and AE−W#A′. The orange spheres denote bond critical points, the yellow spheres denote ring critical points and the green sphere denotes the cage critical point. The all-electron densities in atomic units (a.u.) are displayed for each bond critical point.

Table 2. NCI Parameters[a] of the Most Stable Conformers of CYS−W and AE−W

CYS−W	#A (*g′Gg*)	#B (*gGg*)	#C (*gGt*)	#D (*g′Gg′*)	#A (r_o)	AE−W	#A (*g′Gg*)	#A′ (*g′Gg*)	#D (*g′Gg′*)
BE	−39.2	−37.1	−33.1	−31.3		*BE*	−45.5	−45.2	−38.3
IE	−42.1	−38.5	−34.1	−36.2		*IE*	−49.5	−48.7	−48.8
IE_{SAPT}	−43.3	−39.5	−35.1	−36.7		IE_{SAPT}	−52.5	−51.5	−51.5
d(NO)	1.895	1.895	1.908	1.904	1.953	*d*(N−HO)	1.900	1.907	1.856
d(O−HS)	2.395	—	—	2.231	2.483	*d*(O−HO)	2.010	1.969	1.891
d(O−HC)	2.541	2.459	—	—	2.742	*d*(O−HC)	2.586	2.835	—
ρ(N−HO)	0.0340	0.0341	0.0327	0.0331		ρ(N−HO)	0.0205	0.0224	0.0376
ρ(O−HS)	0.0099	—	—	0.0148		ρ(O−HO)	0.0335	0.0328	0.0279
ρ(O−HC)	0.0076	0.0086	—	—		ρ(O−HC)	—		—

[a] $BE = E_{AB} - (E_A + E_B)$ is the binding energy in kJ mol^{-1} calculated as the difference between the energy of the complex (AB) and the energy of the two isolated constituting units (A and B) in their respective minimum configurations. $IE = E_{AB} - (E_A^* + E_B^*)$ is the interaction energy in kJ mol^{-1} calculated as the difference between the energy of the complex and the energy of the two constituting units at the geometric configuration within the complex (A* and B*). IE_{SAPT} is the interaction energy in kJ mol^{-1} obtained with SAPT analysis (DF-SAPT2+(3)δMP2/aug-cc-pVTZ). *d* is the HB distance in Å. ρ is the electron density at the bond critical point in atomic units.

conformer for CYS−W is the global minimum, #A. On the other hand, the question remains open as to which conformation of AE−W is the global minimum between #A, #A′ or #D or if one of the observed ones[37] should be #A or #A′, or perhaps a geometry which reflects a rapid interconversion between conformers on the time scale of the microwave spectroscopy experiment.

An analysis utilizing both independent gradient models based on Hirshfeld partition (IGMH)[43,44] and quantum theory of atoms-in-molecules (QTAIM)[45] was conducted to get an insight into the intermolecular interactions within CYS−W and compare these with those in AE−W. The IGMH results are summarized in Figure 1, Figure S3 and Figure S4. The surfaces delineated between molecules signify weak interactions (green), strong attractive interactions(blue) and strong repulsive interactions (red). The color scale of these surfaces corresponds to their respective sign(λ_2)ρ as shown more quantitatively in the scatter plots of Figures S3 and S4. As described above, the configuration of the global minimum of CYS−W is #A where the CYS moiety is in the *g′Gg* arrangement and the water molecule is positioned within the interstice, situated between the amino and the thiol groups. Conformer #A contains a strong $O_wH_w\cdots N$ HB and two weaker interactions namely, C1H$\cdots O_w$ and SH$\cdots O_w$. From the scatter plots, the δ_g value for $OH_w\cdots N$ is the highest, approximately 0.056 a.u., while the other two weaker interactions are displayed at values lower than 0.02 a.u. Sulfur is less electronegative than oxygen which leads to the SH$\cdots O_w$ interaction being notably weaker than the $O_wH_w\cdots N$ one. It is consequently possible for the hydrogen atom of the C2H group to form an additional weak interaction with the oxygen atom of water. The same NCIs are present in AE−W but the SH$\cdots O_w$ interaction is replaced by OH$\cdots O_w$ one. While the other NCIs are of similar intensities, the OH$\cdots O_w$ in AE−W is stronger than SH$\cdots O_w$ in CYS−W (δ_g = 0.04 a.u. and 0.02 a.u. in the scatter plots reported in Figures S4(a) and S3(a)) which illustrates that an OH group is more able to form HBs than is an SH group. It is notable that only conformer #A of each of CYS−W and AE−W have the right orientation to form three NCIs suggesting that the weak O$\cdots$HC interaction is essential in stabilizing the global minimum of each complex. Subsequent QTAIM analysis provided additional confirmation of the IGMH calculation results. The analysis of CYS−W revealed three bond critical points as depicted in Figure 3: $OH_w\cdots N$, SH$\cdots O_w$ and CH$\cdots O_w$. The all-electron density of the $OH_w\cdots N$ bond critical point is the highest at 3.40×10^{-2} a.u. The SH$\cdots O_w$ and CH$\cdots O_w$ interactions are weaker with all electron densities of 9.87×10^{-3} and 7.64×10^{-3} a.u. respectively. As also illustrated in Figure 3, AE−W contains an $O_wH_w\cdots N$ hydrogen bond which is of similar strength to the primary bond in CYS−W, and where this interaction and the OH$\cdots O_w$ hydrogen bond have electron densities of 3.35×10^{-2} and 2.05×10^{-2} a.u., respectively.

Binding energies (*BE*) and interaction energies (*IE*) have been calculated at the MP2/aug-cc-pVTZ level. Calculations of the interaction energies by the symmetry-adapted perturbation theory (SAPT) approach (IE_{SAPT})[46] have also been performed (Table 2). The *BE* of CYS−W #A is indeed significantly lower than that of AE−W #A and #A′ (39.2, 45.5 and 45.2 kJ mol^{-1} respectively). The same trend is visible also in the values of *IE*

(42.1, 49.5 and 48.7 kJ mol^{-1} respectively) and the higher values with respect to the *BE*s imply a substantial alteration in the structure of both CYS and AE during complex formation. The higher binding energy of AE−W with respect to CYS−W is further verified by the calculation results obtained from IGMH presented in Figure 3. The OH group of AE displays a significantly stronger interaction with water than the SH group, thereby offering a clear explanation for the higher binding energy observed in its monohydrate structure.

The details of the SAPT calculations are shown in Table S8, where the interaction energy, IE_{SAPT}, is decomposed into four components: electrostatic, induction, dispersion and exchange-repulsion. Among the conformers of CYS−W, the sum of negative components for #A is the largest, and even if the exchange-repulsion energy component for this conformation is large, it still gives the largest value of IE_{SAPT}. Differently, for the AE−W complex, #D has the largest sum of negative components, but the value of its exchange-repulsion energy is much larger than that of #A, making the IE_{SAPT} of #D smaller than that of #A. This shows that in the AE−W #D conformation, the insertion of water is related to a large repulsion term which makes this structure less stable. The difficulty in accommodating the water in AE−W #D is also reflected in the large difference between the *BE* and *IE* (10.5 kJ mol^{-1}) which is the largest for all conformers analyzed. The #A′ conformer, which differs from #A only in the orientation of the free OH group, presents higher values in both the negative and repulsion terms resulting in a slightly lower interaction energy.

Analysis of the rotational spectra of three isotopologues of CYS−W alongside quantum chemical calculations has confirmed the lowest-energy conformer of CYS−W to be as shown for #A in Figure 1. Accurate atom coordinates and other (r_s and pseudo-r_0) structural parameters have been determined. During the present work, theoretically calculated values of some (r_e) structural parameters facilitated a pseudo-r_0 approach which allowed the calculated rotational and NQC constants to be reconciled with those observed experimentally. This allows unequivocal assignment of the observed spectrum to the lowest-energy conformer of the complex (#A). It has further been shown that the conformational surface is shallower for AE−W than for CYS−W such that different theoretical methods give different results as to the identity of the global minimum for AE−W. According to calculations, the lowest-energy conformer of AE−W is similar (in respect of the intermolecular interactions that are present) to CYS−W #A. It is proposed that the global minima in each of CYS−W and AE−W are characterized by three NCIs. The very weak CH···O_w interaction is essential in deciding the global minimum structure of CYS−W and may also make an important contribution to the geometry of the minimum-energy conformer of AE−W. Given the importance of CYS−W and AE−W as prototype examples of small aggregates where the overall PES is the result of multiple, competing, NCIs, these results are important in a wide range of contexts spanning from biochemistry to astrochemistry.

■ ASSOCIATED CONTENT

Supporting Information

The Supporting Information is available free of charge at https://pubs.acs.org/doi/10.1021/acs.jpclett.4c02353.

Experimental and theoretical methods and associated references, tables of experimental transition frequencies, additional tables of experimental and spectroscopic parameters, theoretical equilibrium structure, and additional figures (PDF)

■ AUTHOR INFORMATION

Corresponding Authors

Sonia Melandri − *Dipartimento di Chimica "G. Ciamician", Università di Bologna, 40126 Bologna, Italy;* orcid.org/0000-0002-0410-5833; Email: sonia.melandri@unibo.it

Nicholas R. Walker − *Chemistry - School of Natural and Environmental Sciences, Newcastle University, Newcastle-upon-Tyne NE1 7RU, U.K.;* orcid.org/0000-0002-9450-305X; Email: nick.walker@newcastle.ac.uk

Authors

Wentao Song − *Dipartimento di Chimica "G. Ciamician", Università di Bologna, 40126 Bologna, Italy*

Assimo Maris − *Dipartimento di Chimica "G. Ciamician", Università di Bologna, 40126 Bologna, Italy;* orcid.org/0000-0003-2644-0023

Charlotte N. Cummings − *Chemistry - School of Natural and Environmental Sciences, Newcastle University, Newcastle-upon-Tyne NE1 7RU, U.K.;* orcid.org/0000-0002-1453-2871

Luca Evangelisti − *Dipartimento di Chimica "G. Ciamician", Università di Bologna, 40126 Bologna, Italy;* orcid.org/0000-0001-9119-1057

Complete contact information is available at: https://pubs.acs.org/10.1021/acs.jpclett.4c02353

Notes

The authors declare no competing financial interest.

■ ACKNOWLEDGMENTS

The authors thank the University of Bologna for financial support (RFO) and the CINECA award under the ISCRA initiative, for the availability of high-performance computing resources and support. The support from local research agencies is gratefully acknowledged: S.M., L.E. and A.M. thank the Italian Ministry of Research (PRIN national project, grant no. J43C21000050001). W.S. acknowledges the China Scholarship Council (CSC) and the Marco Polo grant for financial support. The authors acknowledge the Engineering and Physical Sciences Research Council for a DTA studentship awarded to C.N.C. and the European Research Council for project funding (Grant No. CPFTMW-307000).

■ REFERENCES

(1) Ball, P. Water as an Active Constituent in Cell Biology. *Chem. Rev.* **2008**, *108* (1), 74−108.

(2) Matsuno, R.; Dopfer, O.; Fujii, M.; Miyazaki, M. Hydration Rearrangement in the 4-Aminobenzonitrile-(H2O) 2 Cluster Induced by Photoionization: The Effect of Solvent-Solvent Interactions. *Chem. Eur. J.* **2023**, *29* (44), No. e202301128.

(3) Richardson, J. O.; Pérez, C.; Lobsiger, S.; Reid, A. A.; Temelso, B.; Shields, G. C.; Kisiel, Z.; Wales, D. J.; Pate, B. H.; Althorpe, S. C. Concerted Hydrogen-Bond Breaking by Quantum Tunneling in the Water Hexamer Prism. *Science (1979)* **2016**, *351* (6279), 1310−1313.

(4) Spada, L.; Gou, Q.; Geboes, Y.; Herrebout, W. A.; Melandri, S.; Caminati, W. Rotational Study of Dimethyl Ether-Chlorotrifluoro-

ethylene: Lone Pair··· π Interaction Links the Two Subunits. *J. Phys. Chem. A* **2016**, *120* (27), 4939−4943.
(5) Calabrese, C.; Li, W.; Prampolini, G.; Evangelisti, L.; Uriarte, I.; Cacelli, I.; Melandri, S.; Cocinero, E. J. A General Treatment to Study Molecular Complexes Stabilized by Hydrogen-, Halogen-, and Carbon-Bond Networks: Experiment and Theory of $(CH_2F_2)N\cdots(H_2O)_m$. *Angew. Chem., Int. Ed.* **2019**, *58* (25), 8437−8442.
(6) Chen, X.; Wang, G.; Zeng, X.; Li, W.; Zhou, M. Unveiling the Role of Water on π-π Stacking Through Microwave Spectroscopy of (Thiophene) 2-(Water) 1−2 Clusters. *J. Am. Chem. Soc.* **2024**, *146* (2), 1484−1490.
(7) Evangelisti, L.; Brendel, K.; Mäder, H.; Caminati, W.; Melandri, S. Rotational Spectroscopy Probes Water Flipping by Full Fluorination of Benzene. *Angew. Chem.* **2017**, *129* (44), 13887−13891.
(8) Song, W.; Maris, A.; Rivilla, V. M.; Fortuna, F.; Evangelisti, L.; Lv, D.; Rodríguez-Almeida, L.; Jiménez-Serra, I.; Martín-Pintado, J.; Melandri, S. Micro-and Millimeter-Wave Spectra of Five Conformers of Cysteamine and Their Interstellar Search. *Astron. Astrophys.* **2022**, *661*, A129.
(9) Pitari, G.; Maurizi, G.; Flati, V.; Ursini, C. L.; Spera, L.; Duprè, S.; Cavallini, D. Enzymatic Synthesis of S-Aminoethyl-L-Cysteine from Pantetheine. *Biochimica et Biophysica Acta (BBA)-General Subjects* **1992**, *1116* (1), 27−33.
(10) Pitari, G.; Malergue, F.; Martin, F.; Philippe, J. M.; Massucci, M. T.; Chabret, C.; Maras, B.; Duprè, S.; Naquet, P.; Galland, F. Pantetheinase Activity of Membrane-Bound Vanin-1: Lack of Free Cysteamine in Tissues of Vanin-1 Deficient Mice. *FEBS Lett.* **2000**, *483* (2−3), 149−154.
(11) Coloso, R. M.; Hirschberger, L. L.; Dominy, J. E.; Lee, J.-I.; Stipanuk, M. H. Cysteamine Dioxygenase: Evidence for the Physiological Conversion of Cysteamine to Hypotaurine in Rat and Mouse Tissues. *Taurine 6* **2006**, *583*, 25−36.
(12) Atallah, C.; Charcosset, C.; Greige-Gerges, H. Challenges for Cysteamine Stabilization, Quantification, and Biological Effects Improvement. *J. Pharm. Anal* **2020**, *10* (6), 499−516.
(13) Paul, B. D.; Snyder, S. H. Therapeutic Applications of Cysteamine and Cystamine in Neurodegenerative and Neuropsychiatric Diseases. *Front Neurol* **2019**, *10*, 497214.
(14) Gahl, W. A.; Balog, J. Z.; Kleta, R. Nephropathic Cystinosis in Adults: Natural History and Effects of Oral Cysteamine Therapy. *Ann. Int. Med.* **2007**, *147* (4), 242−250.
(15) Markello, T. C.; Bernardini, I. M.; Gahl, W. A. Improved Renal Function in Children with Cystinosis Treated with Cysteamine. *New England Journal of Medicine* **1993**, *328* (16), 1157−1162.
(16) Besouw, M.; Masereeuw, R.; Van Den Heuvel, L.; Levtchenko, E. Cysteamine: An Old Drug with New Potential. *Drug Discov Today* **2013**, *18* (15−16), 785−792.
(17) Farshi, S.; Mansouri, P.; Kasraee, B. Efficacy of Cysteamine Cream in the Treatment of Epidermal Melasma, Evaluating by Dermacatch as a New Measurement Method: A Randomized Double Blind Placebo Controlled Study. *Journal of dermatological treatment* **2018**, *29* (2), 182−189.
(18) Mansouri, P.; Farshi, S.; Hashemi, Z.; Kasraee, B. Evaluation of the Efficacy of Cysteamine 5% Cream in the Treatment of Epidermal Melasma: A Randomized Double-Blind Placebo-Controlled Trial. *British Journal of Dermatology* **2015**, *173* (1), 209−217.
(19) Gahl, W. A. Early Oral Cysteamine Therapy for Nephropathic Cystinosis. *Eur. J. Pediatr* **2003**, *162*, S38−S41.
(20) Tatsuta, M.; Iishi, H.; Yamamura, H.; Baba, M.; Mikuni, T.; Taniguchi, H. Inhibitory Effect of Prolonged Administration of Cysteamine on Experimental Carcinogenesis in Rat Stomach Induced by N-Methyl-N′-Nitro-N-Nitrosoguanidine. *Int. J. Cancer* **1988**, *41* (3), 423−426.
(21) Wang, R. H.; Chen, P. R.; Chen, Y. T.; Chen, Y. C.; Chu, Y. H.; Chien, C. C.; Chien, P. C.; Lo, S. Y.; Wang, Z. L.; Tsou, M. C.; Chen, S. Y.; Chiu, G. S.; Chen, W. L.; Wu, Y. H.; Wang, L. H. C.; Wang, W. C.; Lin, S. Y.; Kung, H. J.; Wang, L. H.; Cheng, H. C.; Lin, K. T. Hydrogen Sulfide Coordinates Glucose Metabolism Switch through Destabilizing Tetrameric Pyruvate Kinase M2. *Nature Communications 2024 15:1* **2024**, *15* (1), 1−18.
(22) Mifsud, D. V.; Kaňuchová, Z.; Herczku, P.; Ioppolo, S.; Juhász, Z.; Kovács, S. T. S.; Mason, N. J.; McCullough, R. W.; Sulik, B. Sulfur Ice Astrochemistry: A Review of Laboratory Studies. *Space Sci. Rev.* **2021**, *217* (1), 14.
(23) Melandri, S.; Maris, A.; Favero, L. B. The Double Donor/Acceptor Role of the NH3 Group: Microwave Spectroscopy of the Aminoethanol-Ammonia Molecular Complex. *Mol. Phys.* **2010**, *108* (17), 2219−2223.
(24) Sun, W.; Schnell, M. Microhydrated 3-Methyl-3-Oxetanemethanol: Evolution of the Hydrogen-Bonding Network from Chains to Cubes. *Angew. Chem.* **2022**, *134* (49), No. e202210819.
(25) Salvitti, G.; Blanco, S.; Lopez, J. C.; Melandri, S.; Evangelisti, L.; Maris, A. Probing Intra-and Inter-Molecular Interactions through Rotational Spectroscopy: The Case of the Odorant 2′-Aminoacetophenone and Its 1:1 Water and Neon Complexes. *J. Chem. Phys.* **2022**, *157* (14), 144303.
(26) Evangelisti, L.; Gou, Q.; Feng, G.; Caminati, W.; Mead, G. J.; Finneran, I. A.; Carroll, P. B.; Blake, G. A. Conformational Equilibrium and Internal Dynamics in the Iso-Propanol-Water Dimer. *Phys. Chem. Chem. Phys.* **2017**, *19* (1), 568−573.
(27) Li, J.; Wang, X.; Zhang, X.; Chen, J.; Wang, H.; Tian, X.; Xu, X.; Gou, Q. Stepwise Hydrations of Anhydride Tuned by Hydrogen Bonds: Rotational Study on Maleic Anhydride-(H_2O) 1−3. *Phys. Chem. Chem. Phys.* **2023**, *25* (6), 4611−4616.
(28) Pracht, P.; Bohle, F.; Grimme, S. Automated Exploration of the Low-Energy Chemical Space with Fast Quantum Chemical Methods. *Phys. Chem. Chem. Phys.* **2020**, *22* (14), 7169−7192.
(29) Calabrese, C.; Maris, A.; Vigorito, A.; Mariotti, S.; Fathi, P.; Geppert, W. D.; Melandri, S. Structure, Dynamics, and Accurate Laboratory Rotational Frequencies of the Acrylonitrile-Methanol Complex. *J. Phys. Chem. A* **2020**, *124* (18), 3601−3608.
(30) Caminati, W.; Millemaggi, A.; Alonso, J. L.; Lesarri, A.; López, J. C.; Mata, S. Molecular Beam Fourier Transform Microwave Spectrum of the Dimethylether-Xenon Complex: Tunnelling Splitting and 131Xe Quadrupole Coupling Constants. *Chem. Phys. Lett.* **2004**, *392* (1−3), 1−6.
(31) Caminati, W.; Evangelisti, L.; Feng, G.; Giuliano, B. M.; Gou, Q.; Melandri, S.; Grabow, J.-U. On the Cl··· C Halogen Bond: A Rotational Study of CF 3 Cl-CO. *Phys. Chem. Chem. Phys.* **2016**, *18* (27), 17851−17855.
(32) Grabow, J.-U.; Stahl, W.; Dreizler, H. A Multioctave Coaxially Oriented Beam-Resonator Arrangement Fourier-Transform Microwave Spectrometer. *Review of scientific instruments* **1996**, *67* (12), 4072−4084.
(33) Balle, T. J.; Flygare, W. H. Fabry-Perot Cavity Pulsed Fourier Transform Microwave Spectrometer with a Pulsed Nozzle Particle Source. *Rev. Sci. Instrum.* **1981**, *52* (1), 33−45.
(34) Zaleski, D. P.; Stephens, S. L.; Walker, N. R. A Perspective on Chemistry in Transient Plasma from Broadband Rotational Spectroscopy. *Phys. Chem. Chem. Phys.* **2014**, *16* (46), 25221−25228.
(35) Pickett, H. M. The Fitting and Prediction of Vibration-Rotation Spectra with Spin Interactions. *J. Mol. Spectrosc.* **1991**, *148* (2), 371−377.
(36) Li, W.; Maris, A.; Calabrese, C.; Usabiaga, I.; Geppert, W. D.; Evangelisti, L.; Melandri, S. Atmospherically Relevant Acrolein-Water Complexes: Spectroscopic Evidence of Aldehyde Hydration and Oxygen Atom Exchange. *Phys. Chem. Chem. Phys.* **2019**, *21* (42), 23559−23566.
(37) Kraitchman, J. Determination of Molecular Structure from Microwave Spectroscopic Data. *Am. J. Phys.* **1953**, *21* (1), 17−24.
(38) Costain, C. C. Determination of Molecular Structures from Ground State Rotational Constants. *J. Chem. Phys.* **1958**, *29* (4), 864−874.
(39) Kisiel, Z. Least-Squares Mass-Dependence Molecular Structures for Selected Weakly Bound Intermolecular Clusters. *J. Mol. Spectrosc.* **2003**, *218* (1), 58−67.

(40) Tubergen, M. J.; Torok, C. R.; Lavrich, R. J. Effect of Solvent on Molecular Conformation: Microwave Spectra and Structures of 2-Aminoethanol van Der Waals Complexes. *J. Chem. Phys.* **2003**, *119* (16), 8397−8403.
(41) Xie, F.; Mendolicchio, M.; Omarouayache, W.; Indira Murugachandran, S.; Lei, J.; Gou, Q.; Eugenia Sanz, M.; Barone, V.; Schnell, M. Structural and Electronic Evolution of Ethanolamine upon Microhydration: Insights from Hyperfine Resolved Rotational Spectroscopy. *Angew. Chem., Int. Ed.* **2024**, DOI: 10.1002/ange.202408622.
(42) Harris, S. J.; Legon, A. C.; Walker, N. R.; Wheatley, D. E. Experimental Detection and Properties of H_2O···Ag-Cl and H_2S···Ag-Cl by Rotational Spectroscopy. *Angew. Chem.* **2010**, *122* (1), 185−187.
(43) Lu, T.; Chen, F. Multiwfn: A Multifunctional Wavefunction Analyzer. *J. Comput. Chem.* **2012**, *33* (5), 580−592.
(44) Lu, T.; Chen, Q. Independent Gradient Model Based on Hirshfeld Partition: A New Method for Visual Study of Interactions in Chemical Systems. *J. Comput. Chem.* **2022**, *43* (8), 539−555.
(45) Bader, R. F. W. A Quantum Theory of Molecular Structure and Its Applications. *Chem. Rev.* **1991**, *91* (5), 893−928.
(46) Jeziorski, B.; Moszynski, R.; Szalewicz, K. Perturbation Theory Approach to Intermolecular Potential Energy Surfaces of van Der Waals Complexes. *Chem. Rev.* **1994**, *94* (7), 1887−1930.